



**University of
Zurich**^{UZH}

**Zurich Open Repository and
Archive**

University of Zurich
University Library
Strickhofstrasse 39
CH-8057 Zurich
www.zora.uzh.ch

Year: 2012

3D microtissue formation of undifferentiated bone marrow mesenchymal stem cells leads to elevated apoptosis

Kelm, J M ; Breitbach, M ; Fischer, G ; Odermatt, B ; Agarkova, I ; Fleischmann, B K ; Hoerstrup, S P

Abstract: Current implantation formats to deliver bone marrow-derived mesenchymal stem cells (MSCs) to the site of myocardial injury resulted only in limited cell retention and integration. As an alternative concept to single cell transplantation, we investigated the fate of cell tracker-labeled syngenic rat MSC microtissue implants, injected into the scar area in a chronic rat myocardial infarction model. Analysis of the explants after 2 and 7 days revealed substantial amounts of the cell tracker within the infarct region. However, the signal was associated with the extracellular matrix rather than with viable implanted cells. Following these results, we systematically evaluated the behavior of MSCs derived from mouse, rat and human origin in the microtissue format in vitro. We found that MSC-composed microtissues of all three species displayed highly elevated levels of apoptotic activity and cell death. This effect could be attenuated by initiating osteogenic differentiation during the tissue formation process. We conclude that MSCs used for tissue regeneration undergo apoptosis in their new environment unless they get appropriate signals for differentiation that permit sustained survival. These findings may explain the limited cellular regeneration potential in current MSC-based clinical trials and may change therapeutic strategies away from pure, un-modulated cell delivery concepts.

DOI: <https://doi.org/10.1089/ten.TEA.2011.0281>

Posted at the Zurich Open Repository and Archive, University of Zurich

ZORA URL: <https://doi.org/10.5167/uzh-51718>

Journal Article

Published Version

Originally published at:

Kelm, J M; Breitbach, M; Fischer, G; Odermatt, B; Agarkova, I; Fleischmann, B K; Hoerstrup, S P (2012). 3D microtissue formation of undifferentiated bone marrow mesenchymal stem cells leads to elevated apoptosis. Tissue Engineering. Part A, 18(7/8):online.

DOI: <https://doi.org/10.1089/ten.TEA.2011.0281>

3D Microtissue Formation of Undifferentiated Bone Marrow Mesenchymal Stem Cells Leads to Elevated Apoptosis

Jens M. Kelm, Ph.D.,^{1,2} Martin Breitbach, Ph.D.,^{3,*} Gregor Fischer, D.V.M.,^{4,*} Bernhard Odermatt, M.D.,⁵ Irina Agarkova, Ph.D.,¹ Bernd K. Fleischmann, M.D.,³ and Simon P. Hoerstrup, M.D., Ph.D.^{1,2}

Current implantation formats to deliver bone marrow-derived mesenchymal stem cells (MSCs) to the site of myocardial injury resulted only in limited cell retention and integration. As an alternative concept to single cell transplantation, we investigated the fate of cell tracker-labeled syngenic rat MSC microtissue implants, injected into the scar area in a chronic rat myocardial infarction model. Analysis of the explants after 2 and 7 days revealed substantial amounts of the cell tracker within the infarct region. However, the signal was associated with the extracellular matrix rather than with viable implanted cells. Following these results, we systematically evaluated the behavior of MSCs derived from mouse, rat, and human origin in the microtissue format *in vitro*. We found that MSC-composed microtissues of all three species displayed highly elevated levels of apoptotic activity and cell death. This effect could be attenuated by initiating osteogenic differentiation during the tissue formation process. We conclude that MSCs used for tissue regeneration undergo apoptosis in their new environment unless they get appropriate signals for differentiation that permit sustained survival. These findings may explain the limited cellular regeneration potential in current MSC-based clinical trials and may change therapeutic strategies away from pure, unmodulated cell delivery concepts.

Introduction

BONE MARROW STROMAL cells (MSCs), also termed mesenchymal stem or progenitor cells, are an adhesive cellular fraction of the marrow with a fibroblastic phenotype in cell culture.¹ Due to a current lack of distinctive markers for MSCs, the overall understanding of their function and phenotype in their physiological environment is limited and based predominantly on *in vitro* data and *in vivo* transplantation studies of labeled or genetically modified MSCs.² Ever since Pereira and coworkers demonstrated the contribution of MSCs in regenerative tissue processes in irradiated mice,³ this cell source has gained increasing attention particularly with regard to their applications in regenerative medicine. They fulfill several characteristics such as self renewal, immunomodulation,⁴ and *in vitro* and *in vivo* differentiation capacity, which makes them highly attractive for cell therapy.⁵ The fact that these cells can be harvested, enriched *in vitro*, and used in an autologous fashion is particularly

appealing for therapeutic purposes. However, to date most cell-based therapeutic approaches using systemic or local delivery routes resulted only in modest integration into injured tissue and consequently only marginal functional improvements have been reported.^{6,7} Moreover, the therapeutic mechanisms of MSCs have remained elusive so far, since the concept of transdifferentiation to, for example, the cardiac lineage could not be clearly proven.⁸ The tissue repairing mechanisms of MSCs are highly debated,⁹ but the most broadly accepted hypothesis is based on paracrine effects triggered by specific factors such as vascular endothelial growth factor (VEGF), fibroblast growth factor-2 (FGF-2), or hepatocyte growth factor (HGF).^{10,11} The importance of understanding the parameters, cytokines, and growth factors directing the fate of MSCs *in vitro* and even more importantly for their therapeutic use under physiological conditions *in vivo* is highlighted by recent findings, displaying osteogenic MSC differentiation and calcification in the infarcted scar tissue in mice.^{12,13} Nevertheless, the survival and

¹Swiss Center for Regenerative Medicine, University of Zurich, Raemistrasse 100, 8091 Zurich, Switzerland.

²Competence Center for Applied Biotechnology and Molecular Medicine, Microscale Tissue Engineering Group, University of Zürich, CH-8057 Zürich, Switzerland.

³Institute of Physiology I, Life & Brain Center, University of Bonn, D-53105, Germany.

⁴Institute of Laboratory Animal Sciences, University of Zürich, CH-8057 Zürich, Switzerland.

⁵Institute of Pathology, University Hospital, CH-8091 Zurich, Switzerland.

*Both authors contributed equally to this work.

temporal persistence after local delivery into injured tissue is a key prerequisite for a therapeutic benefit. A recent study by Müller-Ehmsen and coworkers demonstrated that 34%–80% of the cells are detected immediately after cell injection, but only 0.3%–3.5% could be identified after 6 weeks.¹⁴ Even MSCs immortalized with the human telomerase reverse transcriptase gene (hTERT) showed only low persistence after systemic delivery.¹⁵

In the present study we evaluated the fate of implanted MSC microtissues in a chronic rat myocardial infarct model. Microtissues display a more efficient delivery format than single cell suspensions¹⁶ and indicated good retention of transplanted MSCs. However, the apparently good integration capacity was associated with a high degree of programmed cell death. Consequently, we performed *in vitro* analyses to further elucidate potential mechanisms responsible for the fate of implanted MSCs.

Material and Methods

Mouse and rat bone marrow mesenchymal stem cells (mMSC, rMSC)

MSCs were isolated from transgenic C57Bl/6 mice expressing enhanced green fluorescent protein (EGFP) under control of the ubiquitously active beta-actin promoter¹⁷ or from normal Wistar rats using standard protocols.⁵ Briefly, bone marrow cells from femur and tibia were placed on plastic dishes (Greiner BioOne, Frickenhause, Germany) and the adherent cell fraction grown in minimum essential medium (MEM) alpha (Invitrogen, Carlsbad, CA), supplemented with 10% fetal calf serum (FCS; PAA Laboratories, Linz, Austria).

Human bone marrow-derived mesenchymal stem cells (hMSC)

Bone marrow aspirates were obtained during routine orthopedic surgical procedures involving exposure of the iliac crest, after informed consent (kindly provided by I. Martin). Marrow aspirates (20 ml volumes) were harvested using a bone marrow biopsy needle inserted through the cortical bone; aspirates were immediately transferred into plastic tubes containing 15,000 IU heparin.¹⁸ The adherent cell fraction was cultured as described above. All experiments were performed in accordance to the Swiss Ethic Law, No. StV 21-2006.

Human artery-derived fibroblasts (hAF)

In order to obtain primary human artery-derived fibroblasts (hAFs), de-endothelialized vessel segments of human arteries were minced and cultivated in a 37°C humidified 5% carbon dioxide (CO₂)-containing atmosphere and Dulbecco's modified Eagle's medium (DMEM, Invitrogen, Carlsbad, CA) supplemented with 10% fetal calf serum and 1% penicillin/streptomycin solution (Invitrogen). Pure hAFs which had migrated out of the tissue pieces after 10–14 days were serially passaged and expanded for 4–6 weeks under aforementioned conditions to desired cell numbers.¹⁹

Human cardiac-derived fibroblasts (hCF)

Tissue samples of the right atrial appendage were collected and transferred in cardioplegic solution. After washing, they were minced and transferred into a 50 ml tube and

washed with Joklik's minimum essential medium (JMEM, Cell Technologies, Lugano, Switzerland). JMEM was aspirated and the tissue pieces taken up in JMEM supplemented with 2.5% trypsin (Invitrogen) and transferred into the spinner flask (at 37°C). To improve cell survival, oxygen was supplied by a needle attached to a 0.2 micron filter. The tissue pieces were digested for 90 min and the remaining clumps separated from the cells by filtering through a polyamide mesh. Cardiomyocytes and fibroblasts were subsequently separated by gravitation as adult cardiomyocytes settle faster than fibroblasts. The supernatant containing mostly cardiac fibroblasts was plated in DMEM supplemented with 10% FCS and 1% penicillin/streptomycin.

Cell culture

MSCs, hAFs, and hCFs were cultured in MEM-alpha supplemented with 10% FCS and 1% penicillin/streptomycin at 37°C and 5% CO₂ in a humidified incubator. Cell culture under hypoxic conditions (1% O₂) was performed using a vinyl anaerobic chamber system (Glove Box, Coy Laboratory Products Inc.).

Characterization of MSCs

Functional differentiation of mouse, rat, and human MSC as well as hAF into adipocytes and osteoblasts was induced using standard protocols as described by Pittenger and coworkers⁵ (see Fig. 1S).

Flow cytometry analysis (FACS) of hMSC was performed for further cell characterization (see Fig. 1S). Briefly, cells were harvested and washed once with cold FACS buffer (PBS, 2% FCS, 0.5 M EDTA, 0.05% sodium azide). The MSCs were resuspended in FACS buffer and stained either with a fluorescent- or non-labeled antibody for 20 min at 4°C in the dark. The cells stained with the non-labeled antibodies were washed once with cold FACS buffer and incubated for 20 min at 4°C in the dark with directly conjugated secondary antibodies. After additional washing with FACS buffer, MSCs were resuspended in phosphate-buffered saline (PBS; Sigma Chemicals, St. Louis, MO) containing 1% paraformaldehyde. Flow cytometric analysis was performed using a FACS Calibur (BD). Data were analyzed using FlowJo software (Tree Star). Positive gates were defined by exclusion of 99.9% of corresponding isotype controls.

Microtissue formation

Monolayer cultures were trypsinized and single-cell suspensions seeded with indicated cell concentrations into 60-well plates (HLA plate, Greiner-Bio One, Frickenhausen, Germany). In order to enable gravity-enforced microtissue formation in hanging drops, the 60-well plates were incubated upside down. Microtissues were produced and maintained in MEM-alpha medium supplemented with 10% FCS and 1% penicillin/streptomycin solution.²⁰ Microtissue size was analyzed for at least 10 microtissues per group by bright-field microscopy with subsequent analysis using image J.

Chronic infarct model

Infarct (*n*=10) or sham operations (*n*=5) were performed in 200 g male Wistar rats (8–9 weeks old). Ligation of the left anterior descending coronary artery was performed in the

intubated rats during isoflurane (Isoflo[®] ad us. Vet., Abbott AG, Baar, Switzerland) anesthesia, as described by Pfeffer and coworkers.²¹ Briefly, after opening the fourth intercostal space the heart was exteriorized and the pericardium was cut. The left anterior descending coronary artery was ligated between the left atrium and the pulmonary outflow tract using a 6.0 silk suture (Vicryl[®] & Ethicon[®], Johnson & Johnson MEDICAL GmbH, Switzerland). The heart was replaced into the thoracic cavity and the chest was immediately closed. At the end of operation, all animals received 0.02 mg/kg subcutaneous buprenorphine (Temgesic[®], Essex Chemie AG, Lucerne, Switzerland) for postoperative analgesia (with subsequent doses every 12 h for the first 3 postoperative days), and 10 mg/kg subcutaneous enrofloxacin (Bayer AG, Leverkusen, Germany) as an antibiotic prophylaxis. Animal experiments were performed in accordance to ethical permission No. 127-2005.

Microtissue implantation

After scar tissue formation for at least 6 weeks, syngeneic rMSC composed microtissues consisting of 5000 cells per microtissue were labeled with 10 μ M ((5-(and -6)-(((4-chloromethyl)benzoyl)amino)tetramethylrhodamine)) (CMTMR) (Invitrogen) for 30 min in 1 ml PBS, pH 7.2 in the dark.

The microtissues were washed two times and resuspended in Hanks's balanced salt solution (HBSS) buffer for injections. After opening the fourth intercostal space the heart was exteriorized and approximately 600 microtissues were injected into the scar area of the infarct using Braun Omnican 50 insulin syringes (U-100, 0.30 \times 8 mm). The total injection volume of 50 μ l was distributed over multiple injection sites.

Immunohistochemistry and TUNEL

Immunohistochemistry was performed on paraffin sections of microtissues using the Ventana Benchmark automated staining system (Ventana Medical Systems, Tucson, AZ) and cleaved Caspase-3 primary antibody (Cell Signaling Technology, Danvers, MA). Primary antibody was detected with the Ventana iVIEW DAB detection kit, resulting in a brown reaction product. Sections were counterstained with hematoxylin and covered with a glass cover slip.

Terminal transferase and biotin-16-dUTP apoptosis detection (TUNEL) was performed on paraffin sections of microtissues according to standard protocols. Briefly, deparaffinized sections were incubated with 3% H₂O₂ to block peroxidase activity. After two washings the specimens were incubated with TdT reaction buffer (Roche Diagnostics GmbH, Penzberg, Germany) for 1 h at 37°C. The reaction was stopped, washed, and incubated with Streptavidin-HRP for 20 min at room temperature and further developed with DAB (Roche Diagnostics GmbH) for 1–2 min.

Quantification of immunohistochemical staining

Paraffin sections of microtissues were stained against cleaved Caspase-3 and images were analyzed using Axiovision Autmess software (Carl Zeiss Microimaging, Oberkochen, Germany). The degree of apoptosis was calculated as a ratio between the area of cleaved Caspase-3 positive cells (brown staining) and living cells area (blue staining of cytoplasm). Statistical analysis was performed using ANOVA and post hoc Tukey-Kramer test.

Immunofluorescence analysis

For immunofluorescence analysis, explants and microtissues were harvested, washed twice in PBS, fixed for 1 h in PBS containing 4% paraformaldehyde and subsequently washed three times for 5 min in PBS. Microtissues were embedded in agarose and prepared for frozen sections. The frozen specimen (10 μ m thick) were washed three times with PBS and further permeabilized for 10 min in PBS containing 0.2% Triton X-100 (Sigma Chemicals). The sections were sequentially incubated with primary antibodies targeting Collagen I (polyclonal rabbit, Cedarlane, Burlington, Canada), Collagen IV (polyclonal rabbit, Cedarlane), Fibronectin (polyclonal rabbit, Sigma Chemicals), Laminin (polyclonal, Sigma Chemicals), sarc. alpha-actinin (monoclonal mouse, Sigma Chemicals) and cleaved Caspase-3 (polyclonal rabbit, Cell Signaling Technology, Danvers, MA) for 5 h at room temperature and the detection antibodies, anti-rabbit Cy2 and anti-mouse Cy5 (Jackson Immunochemicals, West Grove, PA) for an additional 2 h at room temperature. Nuclei were visualized by 4',6-diamidin-2-phenylindol (DAPI) (Sigma Chemicals). The specimens were analyzed by confocal laser scanning microscopy (CLSM; Leica TCS SP5, Leica Microsystems, Glattbrugg, Switzerland).

Caspase-3/7 activity assay

Caspase-3/7 activity assay was performed according to the manufactures protocol (Caspase-Glo[®] 3/7 assay, Promega, Dübendorf, Switzerland). Briefly, for Caspase-3/7 activity 10,000 MSCs were seeded to confluence in 96-well plates and cultured for 2 days or four microtissues, each composed of 2500 MSCs, were grown for 2 days in hanging drops. Caspase-3/7 activity was measured after 2 days in culture with a multiwell plate reader (Biotek Instruments, Winooski, VT) in a 96-well plate by luminescence resulting after adding the Caspase-Glo[®] 3/7 buffer in equal amount to the culture medium.

Statistics

Statistical analysis was performed using an unpaired two-sided student *t*-test to evaluate significance (*p*-value) of the results.

Results

MSC microtissue formation

In contrast to single cells, injected microtissues are more adhesive due to their size and an accelerated extracellular matrix production.^{16,22} Hence, the aggregation into microtissues prior to injection might improve the retention of mesenchymal stem cells in the myocardium. Prior to *in vivo* experiments, we have tested microtissue-forming capacity of rat MSCs by using gravity-induced aggregation. Microtissues comprising 5000 rMSCs were formed within 2 days in hanging drop cultures. The generated microtissues had a diameter of about 200 μ m and come easily through the commonly used injection needles. The microtissues have demonstrated normal tissue morphology without any sign of hypoxia. In accordance with a recent study by Bartosh and coworkers,²³ qualitative immunofluorescence analysis demonstrated the appearance of extracellular matrix components such as collagen I, collagen IV, fibronectin, and laminin after only 2 days in culture, indicative of their adhesive properties (Fig. 2S).

rMSC microtissue implantation

To analyze the integration behavior of rMSC-composed microtissues we used a rat chronic infarct model and injected the microtissues directly into the scar tissue. Microtissue implantation was performed in a syngeneic chronic rat infarct model, at least 6 weeks after ligation of the left descending coronary artery. Overall, approximately 600 fluorescent-labeled microtissues (5000 cells/microtissue grown for 2 days) corresponding to 3×10^6 cells were injected into the scar tissue. In previous experiments it could be demonstrated that myocardial microtissues (composed of neonatal rat cardiomyocytes) integrated within 7 days into the myocardium of rats after intrapericardial injection (22).

Therefore we performed a post-transplantation analysis at 2 ($n=5$; Fig. 1a–e) and 7 days ($n=5$; Fig. 1f–j) after implantation. HBSS was used as control and analyzed accordingly after 2 and 7 days. Because no control group showed any fluorescent signal in the CMTMR-specific wavelength, we illustrate only the 2-day HBSS control results (Fig. 1k–n). The scar region was clearly visible in all groups as shown by thinning of the myocardial wall and reduced number of cardiomyocytes (Fig. 1o). In the microtissue transplanted groups, CMTMR positive areas were clearly visible in the scar tissue after 2 and 7 days (Fig. 1a–j). Already after 2 days, the spherical shape of the microtissues was no longer obvious. In addition, after 2 and 7 days, the fluorescent signal appeared to be not associated with viable MSCs, indicating a

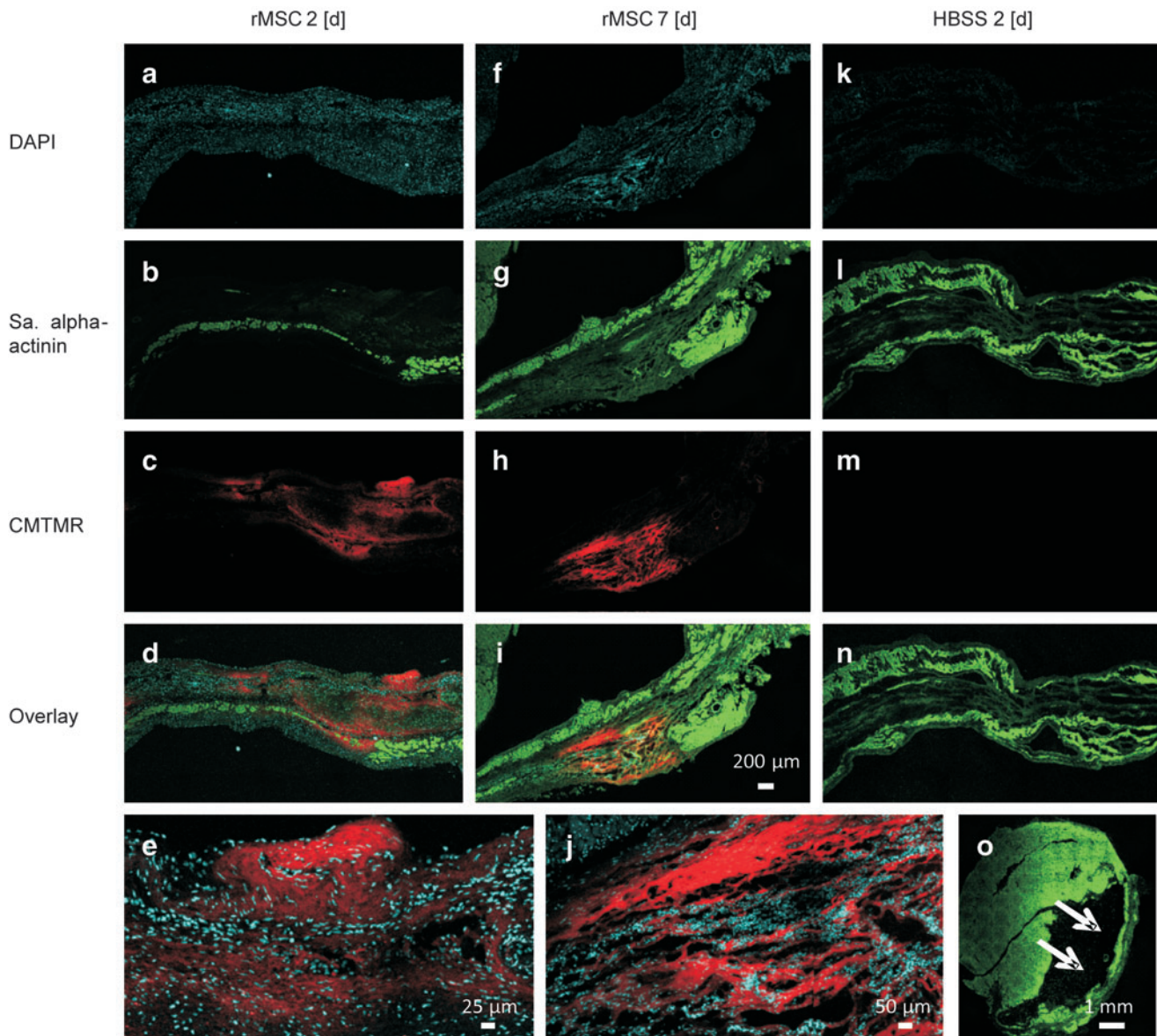


FIG. 1. Appearance of ((5-(and-6)-(((4-chloromethyl)benzoyl)amino)tetramethylrhodamine)) (CMTMR)-labeled rat bone marrow stromal cells (rMSC) microtissues implants 2 days (a–e) and 7 days (f–j) after intramyocardial injection into the chronic scar area. As a control, Hanks's balanced salt solution (HBSS) was injected into the scar area and analyzed after 2 days (k–n). Frozen sections were stained for 4',6-diamidin-2-phenylindol (DAPI) (blue) and sarcomeric alpha actinin (green); CMTMR is shown in red. An overview of the infarcted heart is shown by sarcomeric alpha actinin (green) displaying the reduced wall thickness and cardiomyocyte number in the scar region (o). Color images available online at www.liebertonline.com/tea

high degree of cell death of the implants (Fig. 1e, j). To better understand the observations of the transplantation results, microtissues were systematically analyzed *in vitro* to investigate the MSC behavior after tissue formation.

MSCs survival in microtissue format

Although MSC microtissues retain on the injection site, their survival and persistence might be limited due to cell

death. Therefore, we investigated in more detail whether the tissue formation process of undifferentiated MSCs itself had already had an impact on the survival of the cells. Bone marrow MSCs of mouse, rat, and human origin were re-aggregated to microtissues with indicated cell numbers and observed over time. During a 10-days culture period mMSC-composed microtissues decreased substantially in size and after 10 days no tissues could be detected, independent of the initial cell number (Fig. 2). A similar size profile was

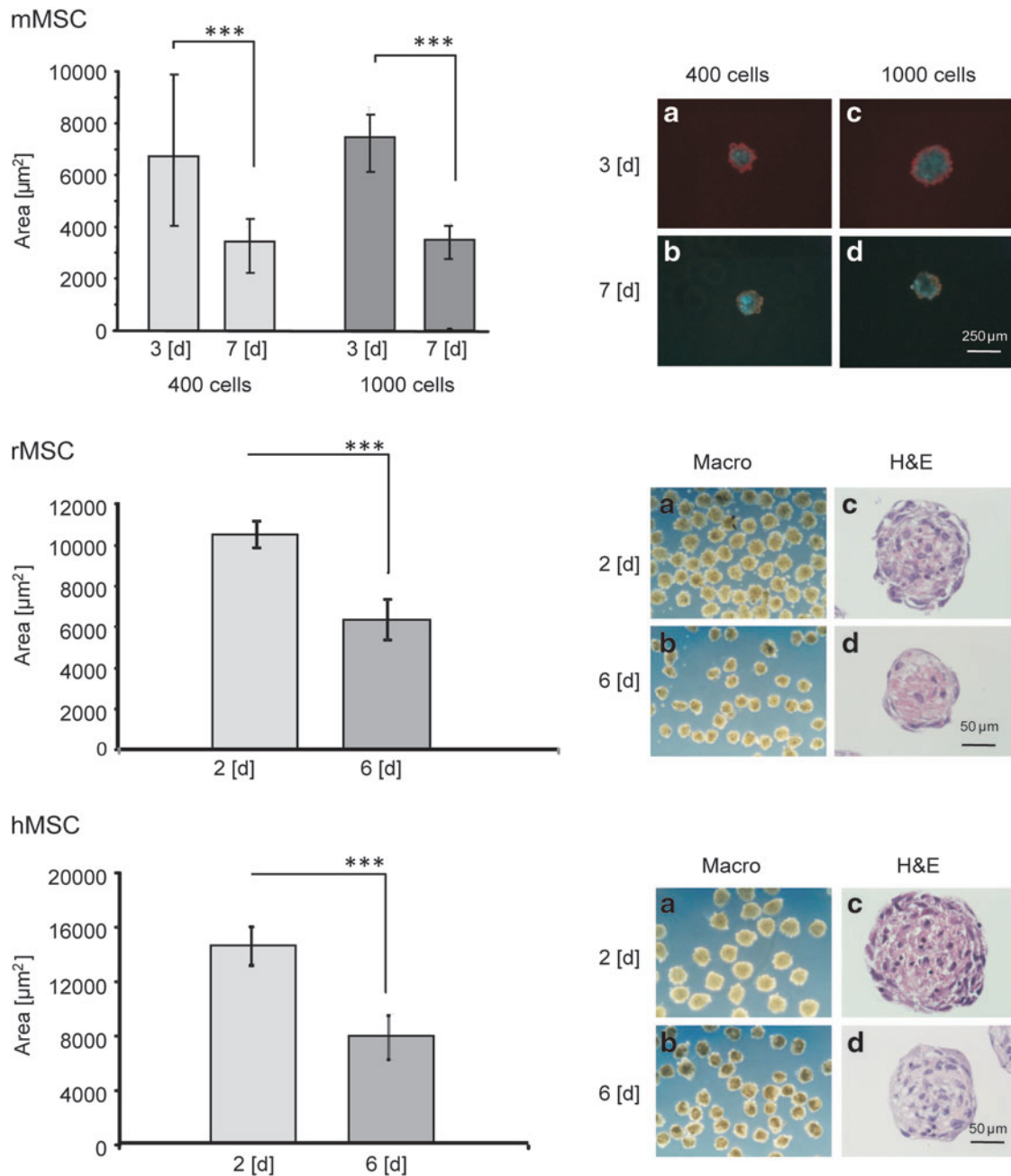


FIG. 2. Size profiling of mouse, rat, and human MSC (mMSC, rMSC, hMSC) microtissues. mMSC-composed microtissues inoculated with 400 and 1000 cells displayed a size reduction of about 40% from day 3 to 7 until after 10 days no tissues could be detected anymore (data not shown). rMSC-composed microtissues inoculated with 2500 cells and hMSC-composed microtissues inoculated with 1000 cells displayed an approximately 40% decrease in diameter between 2 and 6 days in culture. This was confirmed by H&E staining displaying compact microtissues with dying cells. (** $p \leq 0.001$). H&E, hematoxylin and eosin. Color images available online at www.liebertonline.com/tea

observed for the rMSC and hMSC microtissues, where a reduction of about 40% from day 2 to day 6 was measured (Fig. 2). H&E staining of rat and human MSC-microtissue confirmed that the cells form a compact tissue after two days in hanging drop cultures (Fig. 2) with extracellular matrix expression of collagen I, collagen IV, laminin, and fibronectin (shown for rat MSC-microtissue; Fig. 2S).

In order to verify that the decrease in tissue mass is related to cell death rather than tissue disintegration TUNEL analysis was performed in rat and human MSC microtissues. TUNEL-positive cells were not observed in monolayer cultures of rMSCs, hMSCs as well as in hAF control cultures grown for 6 days (Fig. 3a, d, g). After 6 days microtissues that initially contained 2500 rMSCs displayed a severe loss of cells and exhibited a high number of TUNEL-positive cells (Fig. 3c). Similarly, hMSC microtissues displayed a substantial number of TUNEL-positive cells, which could be localized throughout the microtissues (Fig. 3f). In control microtissues composed of artery-derived fibroblasts, TUNEL positive cells could not be detected, which is in accordance with earlier results where no severe cell death could be observed.⁷

To further determine whether the cells enter apoptosis or necrosis after tissue formation, we performed quantitative analysis of Caspase-3/7 activity. The assay was validated by inducing apoptosis through serum deprivation (0% FCS) and cultivation under hypoxic conditions (1% atmospheric O₂)

with confluent MSC-monolayer cultures (inoculated to confluence with 10,000 cells per well). Both, rMSCs and hMSCs displayed elevated levels of Caspase-3/7 activity after 24 h under these conditions (Fig. 4) proving the functionality of the assay. To compare Caspase activity of rMSCs and hMSCs in monolayer cultures and microtissue format, 10,000 cells were seeded to confluency in a 96-well plate. Correspondingly, four microtissues composed of 2500 cells each were placed into one 96-well plate. Peak levels of Caspase-3/7 activity were observed after 2 days and normalized to the inoculated cell number. MSCs of both species displayed elevated Caspase-3/7 activity after tissue formation (rMSC 582.2 ± 83.32 RLU/1000 cells, hMSC 217.00 ± 12.86 RLU/1000cells) compared to their monolayer counterparts (rMSC 44.09 ± 0.1 RLU/1000 cells, hMSC 54.80 ± 3.72 RLU/1000 cells) (Fig. 4), clearly proving a strongly enhanced rate of apoptosis after tissue formation. Human artery fibroblasts as control cells did not show enhancement of Caspase-3/7 activity in microtissues compared to monolayer cultures, clearly proving that apoptosis is not related to the microtissue culture itself.

MSC microtissue differentiation

Recently it was shown that long-term engrafted MSCs can undergo osteogenic differentiation in infarcted mouse hearts.¹² Therefore, we analyzed the effect of osteogenic differentiation

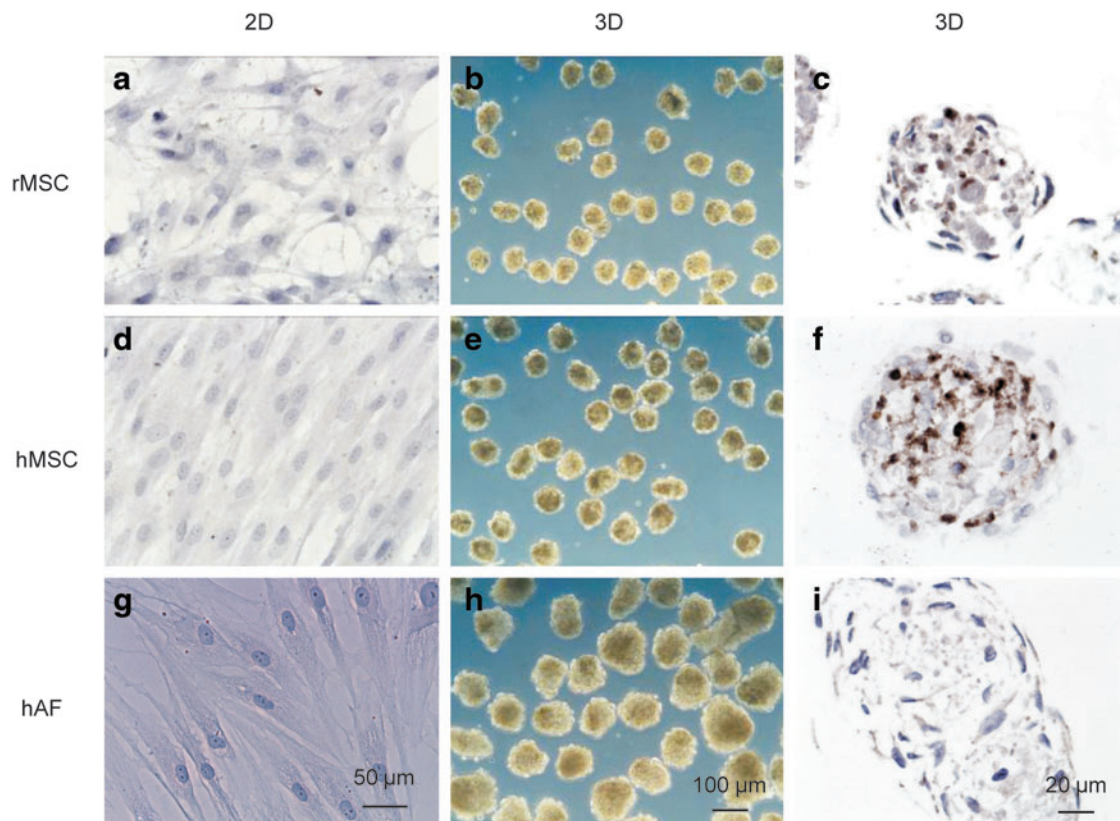


FIG. 3. Terminal transferase and biotin-16-dUTP apoptosis detection (TUNEL) assay of rMSCs (a–c), hMSC (d–f), and arterial-derived control fibroblasts (g–i) grown in monolayer and microtissues after 6 days in culture. Note the prominent amount of TUNEL positive cells (black) in MSC microtissues compared to controls. Color images available online at www.liebertonline.com/tea

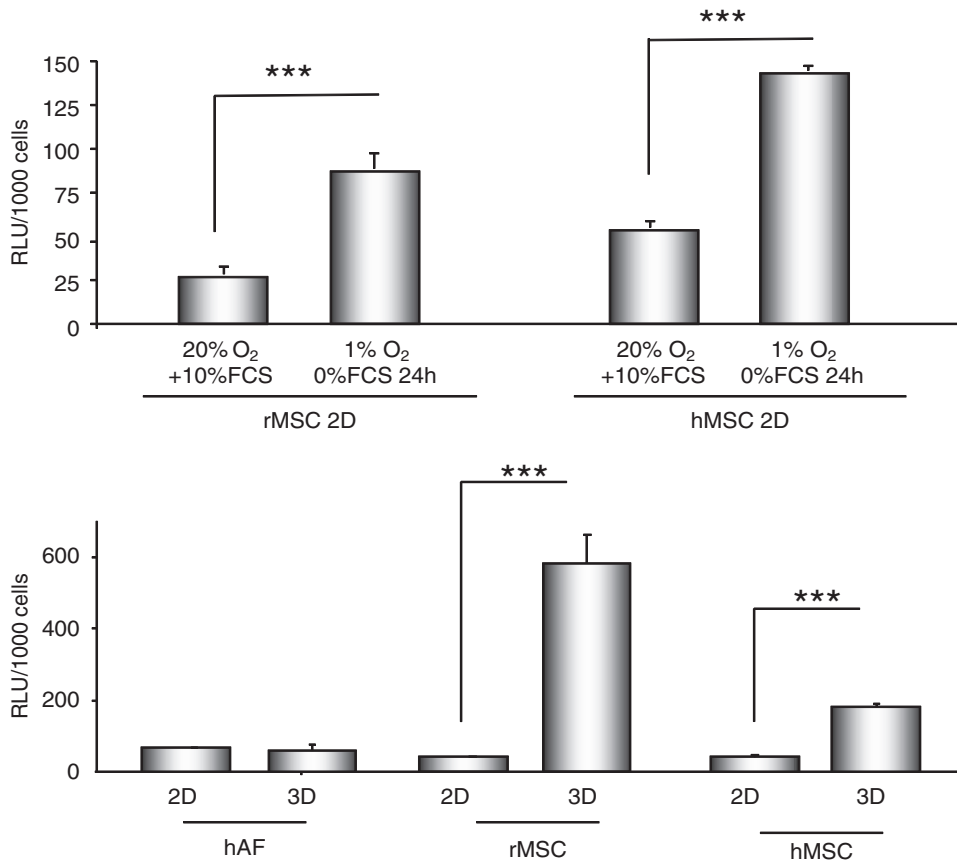


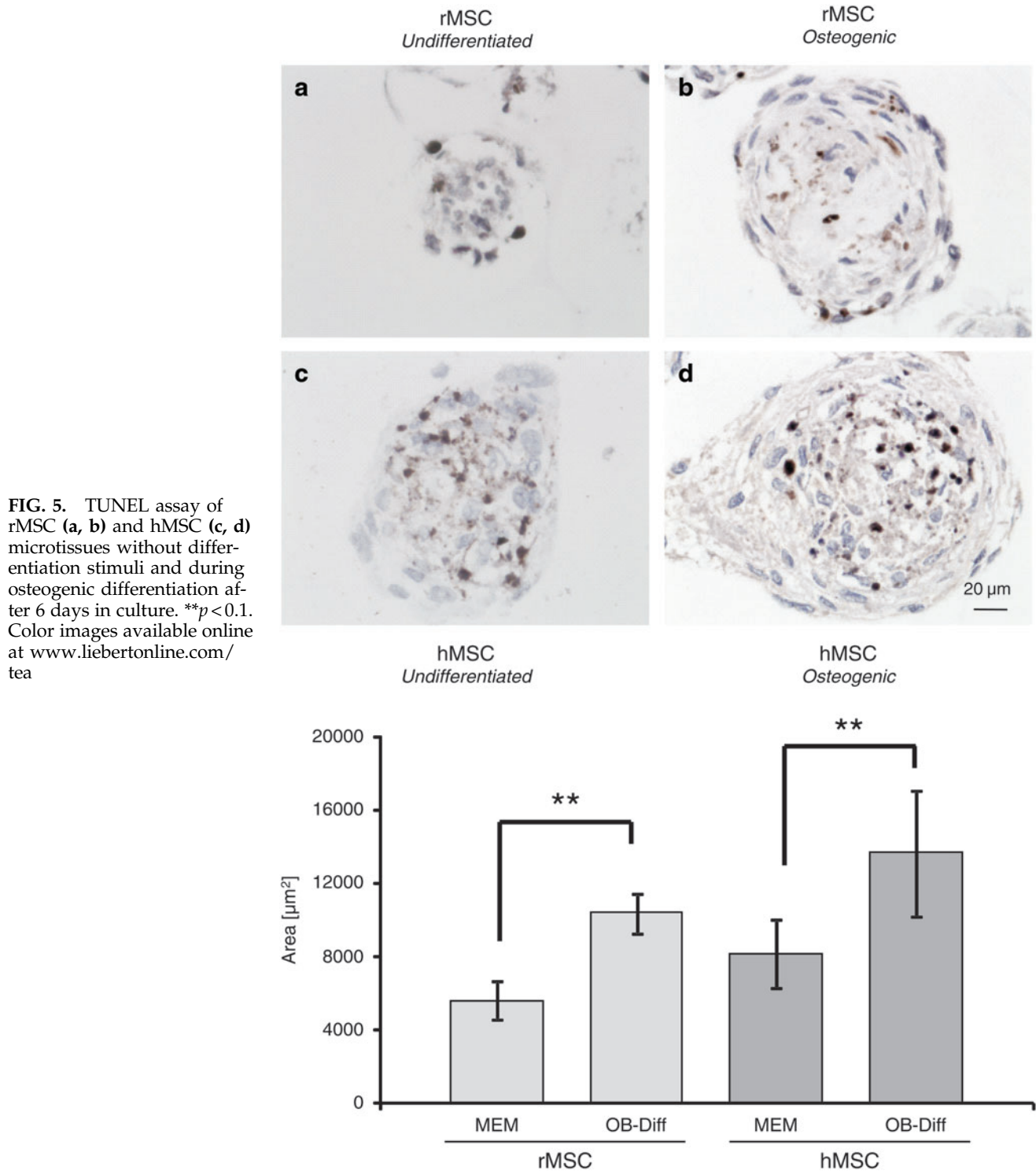
FIG. 4. Caspase-3/7 activity of rMSC, hMSC, and hAF (human artery-derived fibroblast) monolayer and micro-tissue cultures. To confirm the assay apoptosis was induced by growing rMSCs and hMSCs under serum depletion and hypoxia (1% O₂ for 24 h). Increased Caspase-3/7 activity was measured in both MSC-composed micro-tissues in comparison to the monolayer cultures though the effect was more prominent in the rMSC microtissue cultures. Control human artery-derived fibroblasts displayed no difference in Caspase 3/7 activity in both culture formats. (***) $p < 0.01$. FCS, fetal calf serum.

of MSCs in the microtissue format and its impact on their apoptotic activity. MSC microtissues from rat and human origin were grown in osteogenic differentiation medium (ODM). As compared to cells cultured in nondifferentiating medium, rMSCs in ODM displayed an overall lower frequency of cell death after 6 days, as reflected by a lower number of TUNEL-positive cells but also by a sustained tissue appearance (Fig. 5a, b). The cultures of hMSC did not show such a pronounced effect, as under both culture conditions TUNEL positive cells could be detected (Fig. 5c, d). However, under osteogenic conditions a sustained tissue appearance could be observed after 6 days in culture. Cleaved Caspase-3 immunohistochemistry (IHC) staining was used to further corroborate these findings. To validate cleaved Caspase-3 IHC rMSCs were grown in serum depleted medium under hypoxic conditions and under normal culture conditions. The cultures grown under starving conditions displayed upregulated cleaved Caspase-3 in contrast to MSCs cultured under normal conditions (Fig. 6a, b). In the microtissue format, increased levels of cleaved Caspase-3 were detected in MSC microtissues of rat and human origin without inducing osteogenic differentiation (Fig. 6). In contrast, MSC microtissues of both species grown under osteogenic differentiation conditions markedly attenuated cleaved Caspase-3 levels (Fig. 6). Control microtissues produced from human fibroblasts isolated from the artery and the right atrial appendage displayed only low levels of cleaved Caspase-3 (Fig. 6), clearly proving that apoptosis is a specific feature of MSCs cultivated in microtissues and not related to the microtissue culture process per se.

Discussion

Autologous MSCs represent a promising cell source for cell-based therapies; however, although they are already used in clinical trials, the current knowledge is limited with regard to the biological mechanisms involved in their regenerative and healing capacity.

Single cell implantations of MSCs to treat myocardial defects via systemic or intramyocardial applications have provided limited therapeutic benefits; this may be also related to the fact that long term engraftment of these cells within the heart was found to be rather low.^{7,24} Thus, efficient integration, cell survival and persistence appear important for future implementation of MSCs in cell-based therapies, regardless whether primarily the cells directly and/or their paracrine action cause their therapeutic effect. The impact of prolonged MSC survival was demonstrated by Noiseux and coworkers who implanted Akt overexpressing MSCs, which resulted in superior improvement of heart functionality.²⁵ MSC-composed microtissues enhance cellular retention and integration due to their lower motility and higher adhesivity compared to single cells^{7,16,22,26} and are therefore an attractive application format to improve cell-based therapeutic effects. This is also supported by other studies reporting that MSCs grown as spheroids in hanging drops displayed increased therapeutic properties such as anti-inflammatory effects, suggesting that this application format for MSCs is superior to single cell suspensions.^{23,27} Nevertheless, survival and long term engraftment appears to be key for



achieving optimal therapeutic effects. Detailed analysis of the cell fate *in vitro* demonstrated that MSCs form a microtissue already within 2 days, but soon after formation MSC microtissues displayed elevated numbers of apoptotic cells. To exclude that this is not due to the microtissue culture format we also evaluated other cell types of mesenchymal origin such as fibroblasts isolated from the artery and the atrial appendage and did not find increased rates of apoptosis of these cells compared to adherence cultures. This is fully in

accordance with other microtissue types derived from differentiated cells where this effect could not be observed.²⁶

The MSC-specific behavior might be explained by changes in their microenvironment. In their biological niche they are embedded in a complex environment composed of marrow stromal cells, hematopoietic cells, fibroblasts, macrophages, adipocytes, osteoblasts, osteoclasts, and endothelial cells,²⁸ providing the necessary biological cues for maintained survival in an undifferentiated state. Once MSCs are either

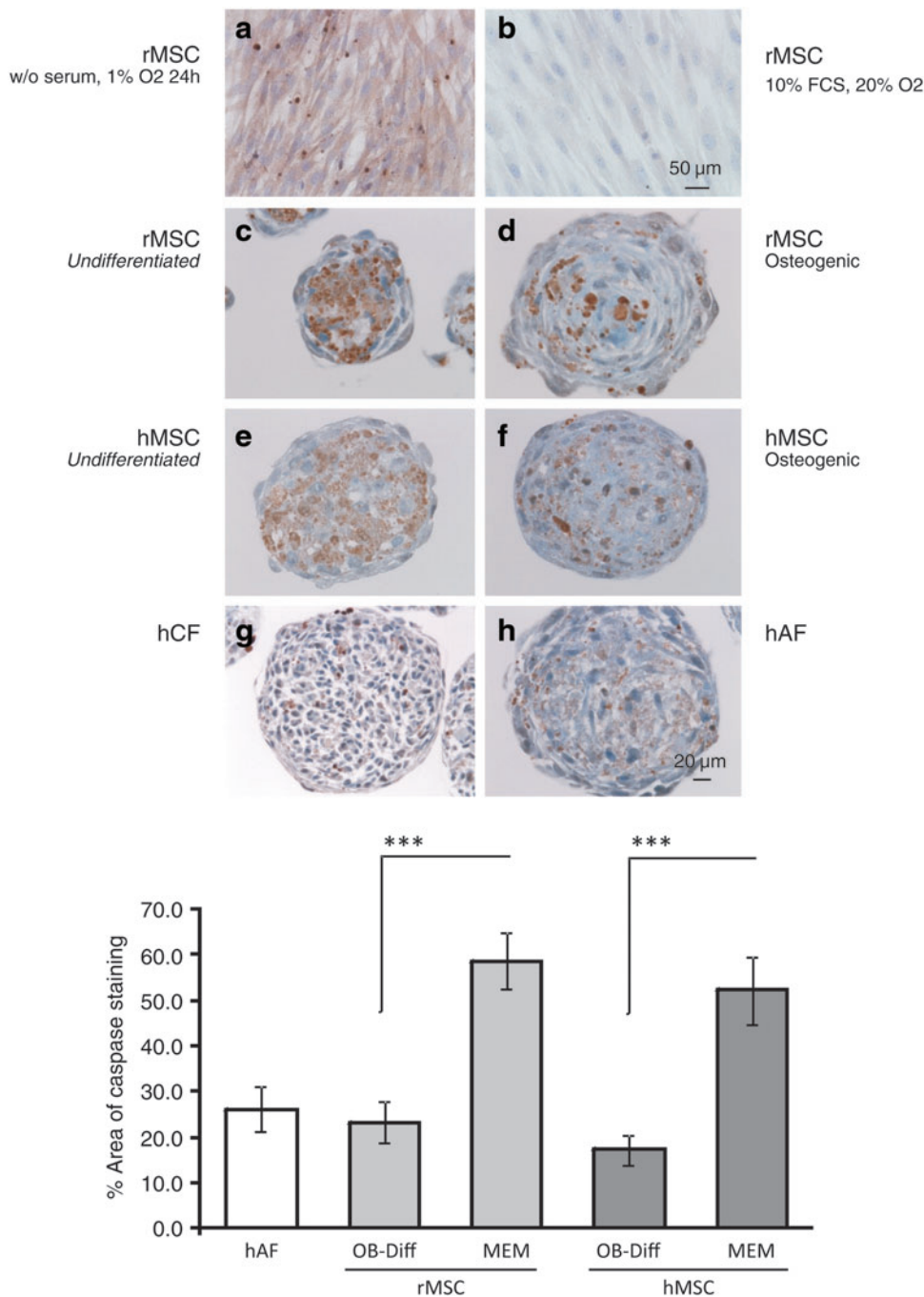


FIG. 6. Immunohistological analysis of cleaved Caspase-3 (shown in brown) was confirmed by induction of apoptosis of rMSC monolayer cultures grown under serum depletion and hypoxia (1% O₂ for 24 h) (**a, b**). Cleaved Caspase-3 was increased in microtissue cultures of rMSC (**c-f**) and hMSC (**g, h**) without differentiation stimuli after 6 days in culture. In microtissues cultures harboring osteogenic differentiation stimuli cleaved Caspase-3 was clearly reduced. Microtissues composed of control cardiac and artery-derived fibroblasts displayed marginal cleaved Caspase-3 levels. The quantification analysis of cleaved Caspase-3 stainings shows significant reduction of the number of apoptotic cells in the microtissues grown in osteogenic differentiation media for both rat and human MSCs. (***) $p \leq 0.001$. Color images available online at www.liebertonline.com/tea

mobilized and home to the injured sites or are expanded *ex vivo* and injected into damaged tissue area, they are confronted with a “nonphysiological” tissue environment involving novel cell–cell contacts, extracellular matrix components, different cell density, physical properties, growth factors, and cytokines. Thus, based on our observations, we hypothesize that in an environment lacking the appropriate biological cues for maintaining their undifferentiated state the MSCs have to differentiate for sustained survival or otherwise undergo apoptosis (Fig. 7). This can be regarded as a biological safety switch to prevent adverse effects of MSCs in ectopic organs. This is substantiated by reports demonstrating that even MSCs transgenic for the pro-survival gene serin/threonine protein kinase 3 (Akt3), which displayed an

improved survival after 3 and 7 days after intramyocardial implantation, could hardly be detected after 14 days.²⁵

The lack of specific MSC markers and thus the ability to evidently monitor only viable MSCs *in vivo* limits relevant follow up investigations with regard to long term survival. Terrovitis and coworkers demonstrated that the survival rate of iron particle loaded stem cells monitored by magnetic resonance imaging resulted in an overestimation of cell survival.²⁹ A low integration and/or survival rate of MSCs in various tissues was summarized by Karp and Teo, demonstrating an average integration rate of far less than 1% (6). Thus, almost no adverse effects have been detected following cellular infusions either intravenously, intraperitoneally, or intramuscularly, most likely due to the short and not

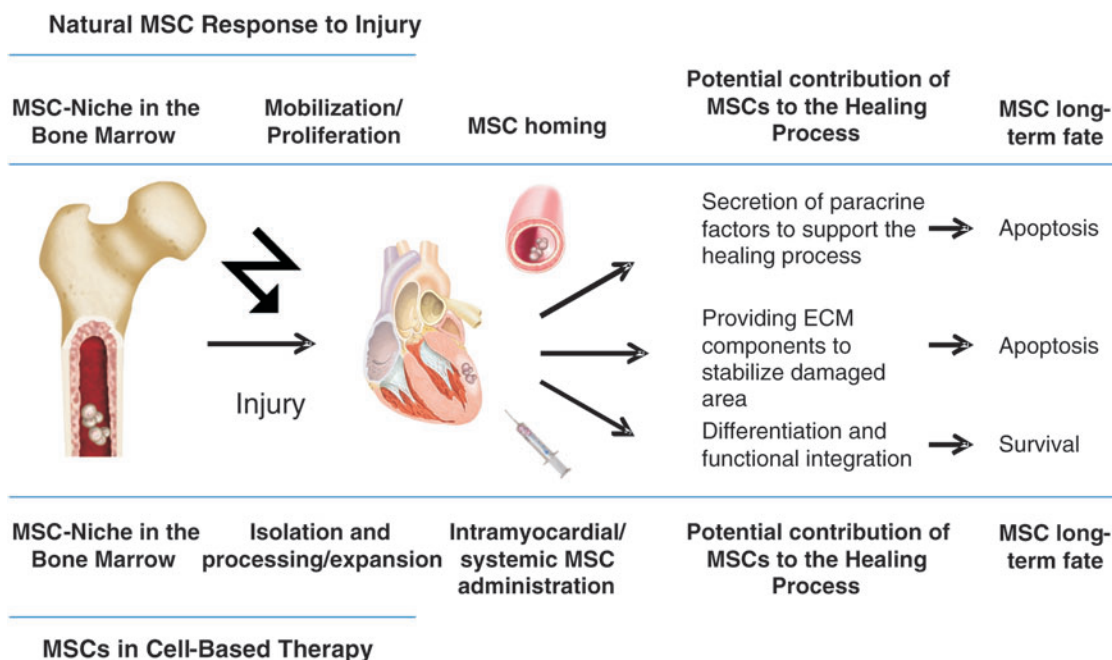


FIG. 7. Hypothesis for a biological safety switch of MSCs mobilized and after systemic or intramyocardial injection. Bone marrow-derived MSCs might contribute to the healing process either by the secretion of paracrine factors, by providing extracellular matrix compounds or by functional differentiation. However, the time window allowed for the secretion of regenerative constituents is rather short. Consequently, MSCs which fall into environment outside of their biological niche and lack the corresponding biological cues for differentiation undergo apoptosis to reduce the risk of tumor formation. Only successful functional differentiation of the MSCs guarantees their long-term survival in the target tissue. Color images available online at www.liebertonline.com/tea

persistent engraftment of undifferentiated MSCs.³¹ On the other hand, observations of long term engraftment were associated with differentiation of MSCs such as osteogenic differentiation leading to calcifications in the heart¹² or the formation of osteosarcomas.³¹ At this, the rigid scar tissue could potentially serve as differentiation stimulus towards the osteogenic lineage.^{13,32} Furthermore, predifferentiation strategies have been shown to improve persistence in bone tissue after intravenous application of the cells.³³

These findings together with earlier investigations may explain in principle the limited cellular regeneration potential of current MSC-based clinical trials and may change the therapeutic strategies away from concepts simply delivering undifferentiated single cell suspensions. Improved survival and persistence of MSCs and the retention capacity of microtissues in combination with predifferentiation strategies might lead to more efficient MSC-based therapies. However, further evaluation of MSCs in their native environment and after integration into injured tissue is required to gain deeper insight into the biology of MSCs and their role in healing processes. It is envisaged that a better understanding of the molecular cues involved in determining the fate of MSCs will assist us in the development of new strategies to improve the survival rate of transplanted MSCs and will increase the overall efficacy of stem cell-based therapies.

Acknowledgments

We thank Petra Wolint for her FACS assistance. This work was supported by the Swiss National Fond No. 112200.

Disclosure Statement

No competing financial interests exist.

References

1. Friedenstein, A.J., Chailakhjan, R.K., and Lalykina, K.S. The development of fibroblast colonies in monolayer cultures of guinea-pig bone marrow and spleen cells. *Cell Tissue Kinet* **3**, 393, 1970.
2. Bernardo, M.E., Locatelli, F., and Fibbe, W.E. Mesenchymal stromal cells. *Ann N Y Acad Sci* **1176**, 101, 2009.
3. Pereira, R.F., Halford, K.W., O'Hara, M.D., Leeper, D.B., Sokolov, B.P., Pollard, M.D., *et al.* Cultured adherent cells from marrow can serve as long-lasting precursor cells for bone, cartilage, and lung in irradiated mice. *Proc Natl Acad Sci USA* **92**, 4857, 1995.
4. Uccelli, A., Moretta, L., and Pistoia, V. Mesenchymal stem cells in health and disease. *Nat Rev Immunol* **8**, 726, 2008.
5. Pittenger, M.F., Mackay, A.M., Beck, S.C., Jaiswal, R.K., Douglas, R., Mosca, J.D., *et al.* Multilineage potential of adult human mesenchymal stem cells. *Science* **284**, 143, 1999.
6. Karp, J.M., and Leng Teo, G.S. Mesenchymal stem cell homing: the devil is in the details. *Cell Stem Cell* **4**, 206, 2009.
7. Kelm, J.M., Lorber, V., Snedeker, J.G., Schmidt, D., Broggini-Tenzer, A., Weisstanner, M., *et al.* A novel concept for scaffold-free vessel tissue engineering: self-assembly of microtissue building blocks. *J Biotechnol* **148**, 46, 2010.
8. Laflamme, M.A., and Murry, C.E. Regenerating the heart. *Nat Biotechnol* **23**, 845, 2005.

9. Prockop, D.J. Repair of tissues by adult stem/progenitor cells (MSCs): controversies, myths, and changing paradigms. *Mol Ther* **17**, 939, 2009.
10. Caplan, A.I., Dennis, J.E. Mesenchymal stem cells as trophic mediators. *J Cell Biochem* **98**, 1076, 2006.
11. Gneocchi, M., He, H., Noiseux, N., Liang, O.D., Zhang, L., Morello, F., *et al.* Evidence supporting paracrine hypothesis for Akt-modified mesenchymal stem cell-mediated cardiac protection and functional improvement. *FASEB J* **20**, 661, 2006.
12. Breitbach, M., Bostani, T., Roell, W., Xia, Y., Dewald, O., Nygren, J.M., *et al.* Potential risks of bone marrow cell transplantation into infarcted hearts. *Blood* **110**, 1362, 2007.
13. Pek, Y.S., Wan, A.C., and Ying, J.Y. The effect of matrix stiffness on mesenchymal stem cell differentiation in a 3D thixotropic gel. *Biomaterials* **31**, 385, 2010.
14. Muller-Ehmsen, J., Krausgrill, B., Burst, V., Schenk, K., Neisen, U.C., Fries, J.W., *et al.* Effective engraftment but poor mid-term persistence of mononuclear and mesenchymal bone marrow cells in acute and chronic rat myocardial infarction. *J Mol Cell Cardiol* **41**, 876, 2006.
15. Bentzon, J.F., Stenderup, K., Hansen, F.D., Schroder, H.D., Abdallah, B.M., Jensen, T.G., *et al.* Tissue distribution and engraftment of human mesenchymal stem cells immortalized by human telomerase reverse transcriptase gene. *Biochem Biophys Res Commun* **330**, 633, 2005.
16. Wang, W., Itaka, K., Ohba, S., Nishiyama, N., Chung, U.I., Yamasaki, Y., *et al.* 3D spheroid culture system on micro-patterned substrates for improved differentiation efficiency of multipotent mesenchymal stem cells. *Biomaterials* **30**, 2705, 2009.
17. Okabe, M., Ikawa, M., Kominami, K., Nakanishi, T., and Nishimune, Y. 'Green mice' as a source of ubiquitous green cells. *FEBS Lett* **407**, 313, 1997.
18. Frank, O., Heim, M., Jakob, M., Barbero, A., Schafer, D., Bendik, I., *et al.* Real-time quantitative RT-PCR analysis of human bone marrow stromal cells during osteogenic differentiation *in vitro*. *J Cell Biochem* **85**, 737, 2002.
19. Hoerstrup, S.P., Zund, G., Schoeberlein, A., Ye, Q., Vogt, P.R., and Turina, M.I. Fluorescence activated cell sorting: a reliable method in tissue engineering of a bioprosthetic heart valve. *Ann Thorac Surg* **66**, 1653, 1998.
20. Kelm, J.M., Timmins, N.E., Brown, C.J., Fussenegger, M., and Nielsen, L.K. Method for generation of homogeneous multicellular tumor spheroids applicable to a wide variety of cell types. *Biotechnol Bioeng* **83**, 173, 2003.
21. Pfeffer, M.A., Pfeffer, J.M., Fishbein, M.C., Fletcher, P.J., Spadaro, J., Kloner, R.A., *et al.* Myocardial infarct size and ventricular function in rats. *Circ Res* **44**, 503, 1979.
22. Kelm, J.M., Djonov, V., Hoerstrup, S.P., Guenter, C.I., Ittner, L.M., Greve, F., *et al.* Tissue-transplant fusion and vascularization of myocardial microtissues and macro tissues implanted into chicken embryos and rats. *Tissue Eng* **12**, 2541, 2006.
23. Bartosh, T.J., Ylostalo, J.H., Mohammadipoor, A., Bazhanov, N., Coble, K., Claypool, K., *et al.* Aggregation of human mesenchymal stromal cells (MSCs) into 3D spheroids enhances their antiinflammatory properties. *Proc Natl Acad Sci USA* **107**, 13724, 2010.
24. Iso, Y., Spees, J.L., Serrano, C., Bakondi, B., Pochampally, R., Song, Y.H., *et al.* Multipotent human stromal cells improve cardiac function after myocardial infarction in mice without long-term engraftment. *Biochem Biophys Res Commun* **354**, 700, 2007.
25. Noiseux, N., Gneocchi, M., Lopez-Illasaca, M., Zhang, L., Solomon, S.D., Deb, A., *et al.* Mesenchymal stem cells over-expressing Akt dramatically repair infarcted myocardium and improve cardiac function despite infrequent cellular fusion or differentiation. *Mol Ther* **14**, 840, 2006.
26. Kelm, J.M., Ehler, E., Nielsen, L.K., Schlatter, S., Perriard, J.C., and Fussenegger, M. Design of artificial myocardial microtissues. *Tissue Eng* **10**, 201, 2004.
27. Frith, J.E., Thomson, B., and Genever, P.G. Dynamic three-dimensional culture methods enhance mesenchymal stem cell properties and increase therapeutic potential. *Tissue Eng Part C* **16**, 735, 2010.
28. Valtieri, M., and Sorrentino, A. The mesenchymal stromal cell contribution to homeostasis. *J Cell Physiol* **217**, 296, 2008.
29. Terrovitis, J., Stuber, M., Youssef, A., Preece, S., Leppo, M., Kizana, E., *et al.* Magnetic resonance imaging overestimates ferumoxide-labeled stem cell survival after transplantation in the heart. *Circulation* **117**, 1555, 2008.
30. Caplan, A.I. Why are MSCs therapeutic? New data: new insight. *J Pathol* **217**, 318, 2009.
31. Tolar, J., Nauta, A.J., Osborn, M.J., Panoskaltsis Mortari, A., McElmurry, R.T., Bell, S., *et al.* Sarcoma derived from cultured mesenchymal stem cells. *Stem Cells* **25**, 371, 2007.
32. Engler, A.J., Sen, S., Sweeney, H.L., and Discher, D.E. Matrix elasticity directs stem cell lineage specification. *Cell* **126**, 677, 2006.
33. Liao, X., Li, F., Wang, X., Yanoso, J., and Niyibizi, C. Distribution of murine adipose-derived mesenchymal stem cells *in vivo* following transplantation in developing mice. *Stem Cells Dev* **17**, 303, 2008.

Address correspondence to:

Jens M. Kelm
Technoparkstrasse 1
8005 Zürich
Switzerland

E-mail: jens.kelm@insphero.com

Received: May 19, 2011

Accepted: July 18, 2011

Online Publication Date: December 12, 2011